research articles Journal of proteome research

Toward Plasma Proteome Profiling with Ion Mobility-Mass Spectrometry

Stephen J. Valentine,[†] Manolo D. Plasencia,[‡] Xiaoyun Liu,[‡] Meera Krishnan,[‡,§] Stephen Naylor,[||] Harold R. Udseth,[⊥] Richard D. Smith,[⊥] and David E. Clemmer*[,‡]

Predictive Physiology and Medicine, 1424 W. Adams Hill Circle, Bloomington, Indiana 47403, Department of Chemistry, Indiana University, Bloomington, Indiana 47405, Department of Genetics and Genomics, Boston University School of Medicine, Boston, Massachusetts and Division of Biological Engineering and Computational Systems Biology, Massachusetts Institute of Technology, Cambridge, Massachusetts, and Biological Sciences Division and Environmental Molecular Sciences Laboratory, Pacific Northwest National Laboratory, P.O. Box 999, MS: K8−98, Richland, Washington 99352

Received May 15, 2006

Differential, functional, and mapping proteomic analyses of complex biological mixtures suffer from a lack of component resolution. Here we describe the application of ion mobility-mass spectrometry (IMS-MS) to this problem. With this approach, components that are separated by liquid chromatography are dispersed based on differences in their mobilities through a buffer gas prior to being analyzed by MS. The inclusion of the gas-phase dispersion provides more than an order of magnitude enhancement in component resolution at no cost to data acquisition time. Additionally, the mobility separation often removes high-abundance species from spectral regions containing low-abundance species, effectively increasing measurement sensitivity and dynamic range. Finally, collision-induced dissociation of all ions can be recorded in a single experimental sequence while conventional MS methods sequentially select precursors. The approach is demonstrated in a single, rapid (3.3 h) analysis of a plasma digest sample where abundant proteins have not been removed. Protein database searches have yielded 731 high confidence peptide assignments corresponding to 438 unique proteins. Results have been compiled into an initial analytical map to be used -after further augmentation and refinement- for comparative plasma profiling studies.

Keywords: ion mobility spectrometry • proteome profiling • multidimensional separations

Introduction

Mammalian tissues require a supply of nutrients as well as a method for waste removal to maintain an efficient homeostatically driven physiology. These requirements demand proximity (directly or indirectly) between essentially every cell within an organism and the circulatory plasma system.[1] Based on this premise, Anderson has argued that plasma contains signatures from essentially every protein within an organism, including those produced by microorganisms.[1] Furthermore, plasma is routinely and readily obtained.[2] This is attractive for integrative biology approaches because information about change in the plasma proteome can be utilized with important patient information (i.e., patient history, clinician's observations, other diagnostic measurements, etc.) to monitor disease predisposition, onset, diagnosis, progression and treatment, possibly for nearly all disease states.[3] These factors, coupled with abundant plasma protein research,[4] have made it perhaps "the most important" of proteomes for clinical applications.[5]

The enormous potential of absolute and differential plasma profiling has been discussed in some detail;[5−12] however, the challenges and uncertainties associated with such analyses are significant, as evidenced by criticism[13−15] of specific efforts. The complexity of plasma as a proteomics sample has been highlighted in a number of reviews[1,5] and several important issues have been emphasized. In addition to the large number of proteins that are expected to be present, concentrations may vary over many orders of magnitude (e.g., albumin is observed at 10−100 mg·mL^{-1} whereas interleukins may be present at only pg·mL^{-1} abundances).[5] Additionally, protein concentrations within individuals may differ according to diverse factors such as age, gender, ethnicity, genetics, diet, and other environmental elements, making even seemingly simple questions such as "what is normal?" difficult to answer definitively.

In total, these issues raise a significant barrier to plasma proteome profiling. To surmount this barrier many present proteomics approaches rely on time-intensive, brute force strategies. Much of the plasma and serum protein characterization work to date has utilized two-dimensional gel electrophoresis (2-DE).[16−19] The advent of shotgun proteomics with

* To whom correspondence should be addressed. E-mail: clemmer@indiana.edu.
[†] Predictive Physiology and Medicine.
[‡] Indiana University.
[§] Present address, Princeton University.
[||] BUSM and MIT.
[⊥] Pacific Northwest National Laboratory.

10.1021/pr060232i CCC: $33.50

Published on Web 10/04/2006

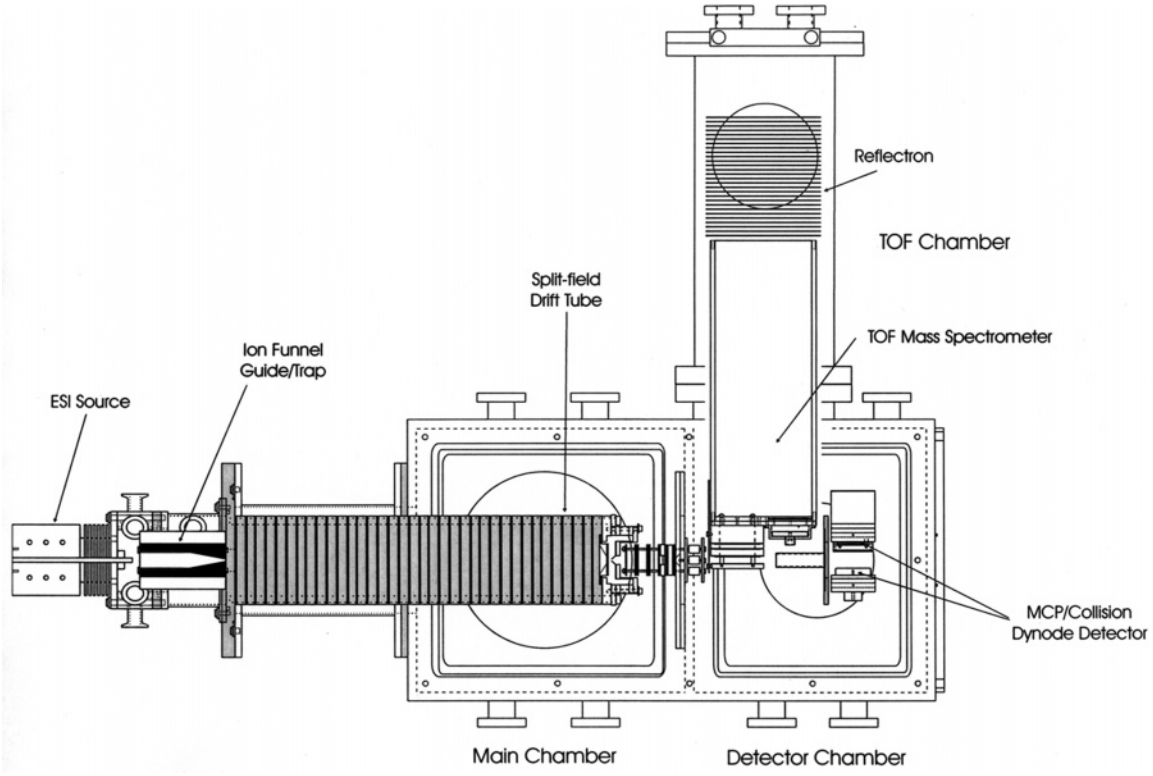

Figure 1. Schematic diagram of the split-field IMS-TOF instrument.

the development of many analytical techniques such as multidimensional separations strategies[20−22] has accelerated the pace of plasma characterization. Recent experiments have combined liquid chromatography with mass spectrometry (LC−MS and LC−MS/MS) techniques to analyze the plasma proteome.[23−27] An expanding repertoire of sample preparation and separations strategies targeting specific proteome regions has also enhanced plasma analysis.[19,24,26−34] An indication of progress is that several hundred plasma proteins had been observed by 2002; however, by 2004, evidence for more than 1600 proteins using LC−MS/MS and 2D LC−MS/MS techniques had been reported.[26] An additional gauge has been the recent report of the Human Proteome Organization (HUPO) presenting evidence for 3020 protein assignments for human plasma of which 889 have recently been determined to be at the 95% confidence limits.[35,36] A goal in plasma proteome profiling is to maximize the coverage as demonstrated in such experiments while minimizing analysis times.

Ion mobility spectrometry (IMS) has been utilized as a rapid gas-phase separations strategy for biomolecular ions.[37−45] The strategy provides high sensitivity because the gas-phase dispersion of peptide ions separates features corresponding to low-abundance species from interfering chemical noise.[46,47] Reduced spectral congestion also allows for the use of shorter experimental run times (LC separations) without sacrificing throughput; short analysis time scales are key to measuring the large numbers of samples required to determine normal protein variability prior to realizing individual plasma profiling. Additionally, mobility-dispersed ions can be fragmented and mobility linked to fragment ions without ion loss from precursor mass selection.[48] These advantages have been demonstrated in head-to-head comparisons with conventional LC−MS/MS technology using rapid (21 min) LC gradients.[44] Overall, the IMS-MS approach provided a 3- and 10-fold increase in the number of identified peptides and plasma proteins, respectively.[44]

The present work reports IMS-MS experiments for a plasma digest sample subjected to two dimensions of LC separation [strong cation exchange (SCX) and reversed-phase (RP) LC]. No effort has been attempted to remove abundant proteins. *From an analysis of the data,* we find evidence for 731 unique peptide ions (hits from MS and MS/MS searches of protein databases) from 438 proteins for the ∼3 h experiment. Comparisons of the observed proteins with the high-confidence list[36] generated from the HUPO dataset[35] showed a relatively *substantial* number (127) of overlapping proteins. Interestingly, many high-confidence proteins observed with the IMS approach are not observed in the HUPO dataset (see below). Results from the present study, combined with those from the previous comparison studies mentioned above, suggest that LC−IMS-MS analyses offer an attractive approach for the rapid profiling of hundreds of human plasma proteins. Current capabilities, limitations, and future directions of the novel IMS-MS approach are discussed.

Experimental Section

Overview: IMS-MS Methods and Instrumentation. In addition to its use as a separations method for gas-phase biomolecular ions, IMS has been used as a structural probe[49−54] and several recent reviews[55−59] describe IMS techniques and their applications in detail. The instrumentation used for the experiments reported here is described in detail elsewhere;[60,61] only a brief description of the IMS-MS method and instrumentation components is given below. A schematic diagram of the ion mobility instrument used for these studies is shown in Figure 1. Briefly, peptides eluting from the pulled-tip capillary column are electrosprayed into an ion funnel similar

to one reported by Smith and co-workers.[62,63] At the back of the funnel, ions accumulate, are stored, and are pulsed (100 μs duration) into the drift tube to initiate mobility measurements. The drift tube employs a split-field design[60] that utilizes two field regions and is filled with 2.60 and 0.12 Torr He and N_2 buffer gases, respectively.

The first field region is ~59 cm long and contains equally spaced electrostatic lenses to generate a uniform field (11.67 V·cm^{-1}). Ions traverse this region under the influence of the electric field and are separated based on their mobilities through the buffer gas. Under low-field conditions, the mobility (K) of an ion through the buffer gas is given as $K = v_D \cdot E^{-1}$ (v_D is the drift velocity of the ion and E is the electric field).[64] Often, to permit comparison between different measurements, it is useful to convert values into reduced mobilities (K_0) by using the relation[64]

$$K_0 = \frac{L^2}{t_D \cdot V} \times \frac{273.2}{T} \times \frac{P}{760}.$$

In this expression, t_D, L, V, P, and T correspond with the measured drift time, length of the drift region, the applied drift voltage, and the pressure and temperature of the buffer gas, respectively. IMS measurements are substantially more reproducible than LC retention times. Any two measurements typically agree to within ~1% (relative uncertainty). Ions that adopt compact conformations have higher mobilities than those that exist as extended conformers.[56−59] For ions of similar size, those that exist as higher charge states will have higher mobilities because they are influenced by a greater drift force.[56,57,65,66]

The second mobility region is ~1 cm long (see Figure 1) and can be modulated between conditions that favor transmission of precursor ions and those that induce ion fragmentation.[60] Because fragment ions originating from the same precursor are coincident in drift time and retention time, it is possible to correlate fragments with the mobility dispersed precursor ions from a single experimental sequence. This has been termed parallel collision-induced dissociation (CID).[67] Throughout the course of a LC experiment, modulation between parent ion and fragment ion conditions is accomplished with fast, high-voltage operational amplifiers (Apex Microtechnology). For these experiments, 2 and 3 s intervals have been used for the collection of parent and fragment ion data, respectively. The total drift time [t_D*(total)*] of an ion is a composite of its transit times in the first and second field regions of the drift tube (t_{D1}, and t_{D2}, respectively). Even though t_{D1} is constant, because of the modulation of the field in the second region, t_{D2} is not. Thus, it is necessary to calibrate t_D*(total)* values between parent and fragment ion datasets to correlate parent ions with fragment ions. This is accomplished with a multipoint calibration using identified peptides.

As ions exit the drift tube, they are focused into the source region of a reflectron-based, time-of-flight (TOF) mass spectrometer. They are pulsed orthogonally into the flight tube to measure their flight times (t_F) in the high vacuum region. Because the flight times are small (μs) compared with drift times (ms) it is possible to collect hundreds of flight time distributions for each packet of ions originating in the ion funnel. Flight times are converted into mass-to-charge (m/z) values for the various ions using a standard calibration procedure.

Plasma Sample Preparation. Pooled plasma samples were donated by the IU school of medicine and stored at −80 °C.[68] A 1.0 mL aliquot was reduced and alkylated using the following procedure. Urea was added to the aliquot to a final concentration of 8 M. Dissulfide bonds were reduced by addition of dithiothreitol (10 mM) and incubation at 37 °C for 2 h. The sample was then alkylated by addition of iodoacetamide (20 mM total concentration) and incubation (in darkness) at 0 °C for 2 h. A 40-fold excess of cysteine was added to quench the reaction. The resulting protein solution was diluted with a phosphate buffered saline (PBS) solution (pH = 7.5) until the urea concentration was 2 M and then digested by adding TPCK-treated trypsin at a 1:50 ratio (trypsin:total protein, incubated at 37 °C for more than 24 h). Tryptic peptides that are produced are desalted with C4 Extraction Columns (J. T. Baker, Inc., Phillipsburg, NJ) and subsequently vacuum-dried. Approximately 400 μg (determined by Bradford assay) of sample was introduced onto the SCX column (see below) for fractionation. A total volume of 6.0 microliters (~240 ng of peptide) was loaded onto the LC column for analysis of each SCX fraction.

Strong-Cation Exchange Fractionation. The SCX fractionation of tryptic peptides was accomplished with a standard HPLC system (600 pump and 2487 dual wavelength detector, Waters Inc., Milford, MA). A column (100 × 2.1 mm) packed with 5 μm 200 Å polysulfethyl A (PolyLC Inc., Columbia, MD) was used for the separation. A flow rate of 0.2 mL·min^{-1} was used to fractionate the sample (~400 μg peptide determined by Bradford assay) into 96-well plates over 1 min intervals with the following gradient: 0% B for 5 min, 0−20% B in 40 min, 45−90% B in 45 min, 90−100% B in 10 min, 100% B for 10 min [where A = 5 mM potassium phosphate, pH = 3 (75:25 water:acetonitrile); B = 5 mM potassium phosphate, 0.35 M potassium chloride, pH = 3 (75:25 water:acetonitrile)]. The absorbance of the eluting peptides was monitored at λ = 214 nm. Individual wells from the 96 well plates were pooled into 10 fractions, desalted with Oasis HLB cartridges, and dried on a centrifugal concentrator. All dried fractions were stored at −80 °C until analysis.

Nanoflow LC Conditions. Nanoflow reverse-phase separations were performed using an Agilent 1100 CapPump (Agilent Technologies Inc., Palo Alto, CA). Initially peptides were loaded onto a 1.5 cm × 100 μm i.d. trapping column (IntegraFrit from New Objectives Inc., Woburn, MA) packed with 5 μm 200 Å Magic C18AQ (Microm BioResources Inc., Auburn, CA) stationary phase using a flow rate of 4 μL·min^{-1}. The flow was decreased over a 2 min interval such that the flow was 250 nL·min^{-1} after 12 min and was switched onto the separation column. Peptides were separated on a pulled-tip capillary column (a 15 cm long, 75 μm i.d. capillary packed with 5 μm, 100 Å Magic C18AQ) using a two solvent setup (solvent A = 96.95% water, 2.95% acetonitrile, 0.1% formic acid; solvent B = 99.9% acetonitrile and 0.1% formic acid). The separation gradient consisted of 10−20% B over 10 min, 20−30% B over 4 min, and 30−38% B over 7 min. A microflame torch (Microflame Inc., Plymouth, MN) was used to create the pulled-tip capillary column by heating an 18 cm long weighted segment of 75 μm i.d. fused silica (Polymicro Technologies LLC, Phoenix, AZ). Column packing is achieved by infusing a stationary phase, methanol slurry into the pulled-tip column using a pressure of 70 bar.

Data acquisition and Experimental Nomenclature. Differences in the time scales (as noted above) of the different measurements (SCX, LC, IMS, MS) allows the recording of the data in a nested fashion; nested drift(flight) time measurements have been described in detail previously.[69] For features observed in the raw datasets, time values for each separation

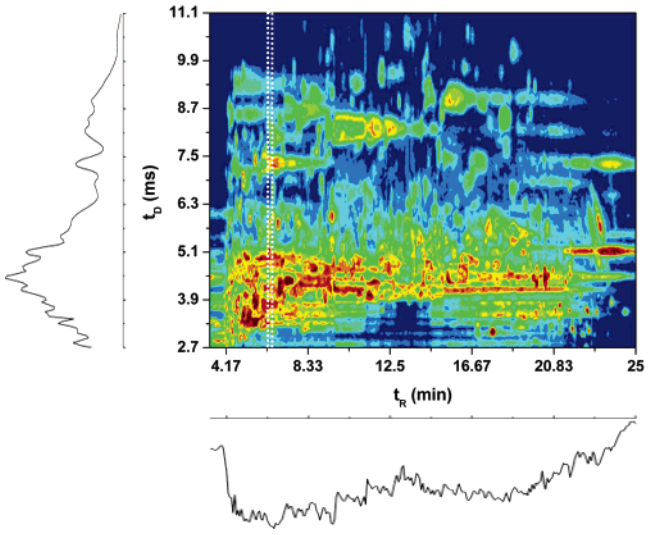

Figure 2. Two-dimensional, $t_R(t_D)$ base-peak plot of a single SCX fraction. A 15 count single bin intensity threshold has been used. On the bottom is the base-peak ion chromatogram obtained by integrating all t_D bins in the 2D base-peak data for each t_R value. On the left is the base-peak drift time distribution obtained by integrating all t_R bins in the 2D base-peak data for each t_D value. The dashed-line rectangle represents the region of data used to generate Figure 3.

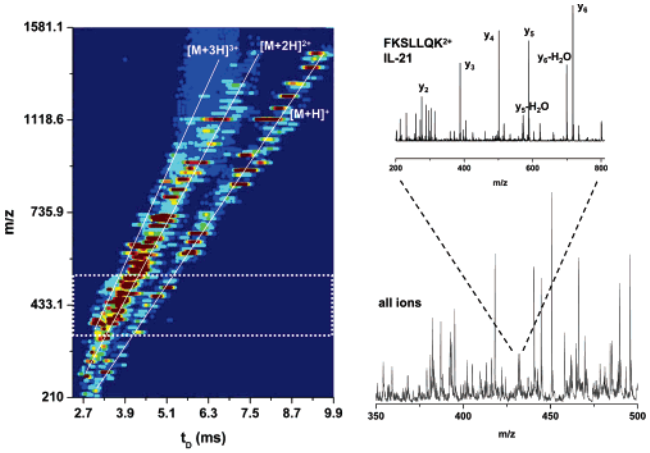

Figure 3. Two-dimensional $t_D(m/z)$ plot (left) obtained for data over a t_R range (Figure 2) of ~25 s. A peak threshold of 15 is used to plot the data. The singly-, doubly-, and triply charged peptide ion families are shown with the white lines. The total-ion mass spectrum (bottom right) obtained by integrating all t_D bins for the indicated m/z values (dashed-line box) is also shown. The MS/MS spectrum for the indicated ion (m/z = 432.26) is shown on top. The assignment of the peptide ion $FKSLLQK^{2+}$ from the protein interleukin 21 is given.

dimension are reported using a standard nomenclature where such values are bracketed in their nesting order.[69,70] For example, features observed in a LC−IMS-TOF dataset would be described with the notation $t_R[t_D(t_F)]$ where t_R is the LC retention time of the peptide. The SCX elution time or fraction number can also be included in the nomenclature,[61] thus the complete nested measurement values would take the form of $t_{SCX}\{t_R[t_D(t_F)]\}$ where t_{SCX} corresponds to the SCX elution time or fraction number.[61]

Results and Discussion

Plasma Digest Data. Figure 2 shows a typical two-dimensional $t_R(t_D)$ base peak plot obtained at a single timepoint (SCX fraction) within the two-dimensional (2D) LC−IMS-MS experiment. From visual inspection of Figure 2, many coeluting (t_R dimension) species are separated based on their mobilities (t_D dimension). The estimated 2D peak capacity shown in Figure 2 is ~6000 (using ~150 and ~40 for the LC and drift dimensions, respectively). Figure 3 shows a two-dimensional, $t_D(m/z)$ plot for data obtained, in this case, over a 25 s t_R window (Figure 2). Within the total-ion mass spectrum (Figure 3), a relatively small peak is observed at a m/z value of 432.26. Selection of such a peak for MS/MS analysis using traditional MS instrumentation is unlikely as many other peaks (at least 20 alone over the mass spectral region shown in Figure 3) are of higher intensity. The parallel CID approach, however, has linked a MS/MS spectrum to this precursor ion to obtain the peptide assignment $FKSLLQK^{2+}$ ($p < 0.007$) from the protein interleukin 21. Overall, the mobility dispersion results in decreased spectral congestion and the mobility-selected MS/MS spectrum (Figure 3) illustrates an advantage of the approach we have taken.

Proteome Map Generation. The base peak plot in Figure 2 is an extremely simplified representation of the data; only the most intense TOF spectral bin at each t_R and t_D value is represented. Typically, for each 21-minute LC gradient run, ~2 to 7 × 10^4 peaks are observed using a relatively high peak threshold (15 counts per 3D bin). The features observed in the precursor and fragment ion datasets obtained from each LC run are used to generate an initial proteome map containing all separation positions (t_{SCX}, t_R, t_D, m/z) as well as peak intensity (I). Figure 4 shows a dot plot illustrating the preliminary map. The positions (t_R, t_D, m/z) for the 6000 most intense features from each SCX fraction are shown. Figure 4 also shows a two-dimensional $t_R(t_D)$, base-peak plot for a single SCX fraction. Intensity information (raised relief color map in Figure 4) is also included in the proteome map. Again, many coeluting features are resolved along the drift axis.

Peak position information is used to correlate fragment ions with precursors, and generate MS/MS files for MASCOT (Matrix Science Ltd., London, UK) database searches[61,71] of the Swiss-Prot[72] nonredundant human database. Peptide assignments are then linked to mapped positions. In total, 6167 unique peptides (3856 proteins) have identity homology scores [i.e., extensive homology or less than 5% probability ($p < 0.05$) of random occurrence]. The initial proteome map thus contains peptide and protein assignments, related MASCOT search information, and peak positions and intensities.

Proteome Map Fidelity: Consideration of False Positives. Although preliminary results are encouraging, it is important to not overstate them. Probability based scoring algorithms, such as that used by MASCOT, often render false positive identifications[73] requiring greater examination of the assigned peptides to create a high-confidence proteome map. This can be accomplished with additional identification criteria. Such constraints may include provisions for the number of fragments observed in a given homologous series, the mass accuracy of priority fragments, as well as the quality of the MS/MS spectra, and perhaps the use of drift time[74,75] and LC retention or elution time[76,77] information. We have generated a high-confidence map by manually inspecting the MS/MS data using the following criteria. Peptide identification requires five or more fragments from a homologous series (primarily b- and y-series ions) with "good" signal-to-noise levels (i.e., putative fragments

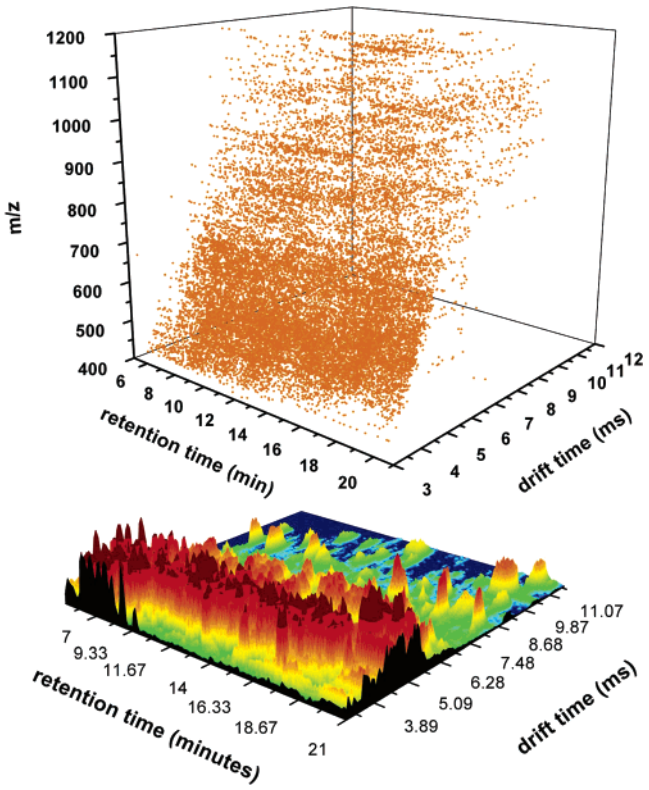

Figure 4. The top plot shows the three-dimensional peak positions obtained from the 6000 most intense features observed in each of the 10 SCX fractions. The bottom plot shows a three-dimensional $t_R(t_D)$ base peak plot obtained from a single SCX fraction. Intensity is shown along the *y*-axis as a raised-relief color map.

are among the dominant MS/MS features). Additionally, the experimental fragment masses fall within ~0.1 Da of theoretical values.[78] *Protein database searches using the LC−IMS-MS data have yielded 731 unique peptide ion assignments (438 proteins).* A complete list of the high-confidence proteins as well as the number of peptide ions observed for each is given in the Supporting Information (provided as a table).

Despite such efforts, it is likely that false positive assignments still exist within the higher confidence map. Figure 5 shows a MS/MS spectrum obtained in the current experiments. Although the spectrum shows assignments for 5 contiguous y-series ions of reasonable signal-to-noise and concordance with theoretical m/z values, the assigned peptide is questionable. Because the sequence shown in Figure 5 is from the signal peptide of the low-abundance protein interleukin 26, it is unlikely that the peptide ion has been observed and, although originally contained within the higher-confidence map, has been removed.

The overall map fidelity can also be described in terms of a false positive rate. The approach employed here uses a nonsense protein database search.[73] MS/MS data for peptide assignments are searched against a reverse protein database generated in house.[79] For the high-confidence map, nonsense database search results have suggested a false positive rate of ~11%. This value is intermediate to the <5% false positive rate reported by MASCOT and the range of false positive rate estimated by HUPO (14.6% to 21.1%).[35] Although the value reported here may be indicative of a minimum rate, we note that each MS/MS spectra had already been visually inspected prior to the search.

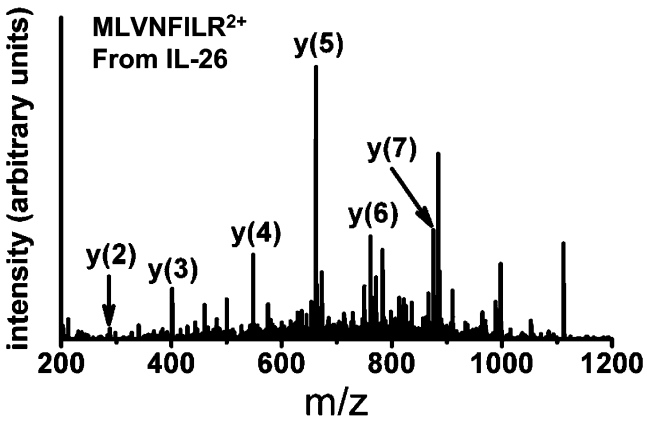

Figure 5. The MS/MS spectrum that provided the assignment for the peptide ion $MLVNFILR^{2+}$ from the protein interleukin 26. The assignment has been obtained from a MASCOT database search. The assignment is highly suspect because the sequence constitutes the signal peptide of the very low-abundant cytokine protein.

Here we note that ~50% of the identified peptides in the current map are unique to given database proteins leading to a large number of proteins identified from a single peptide (see supplementary table). The relatively low sequence coverage of such proteins may in part be attributed to the fact that we have not employed abundant protein removal for these studies. Peptides from proteins such as albumin may mask signals from lower abundance species despite the mobility dispersion. For example, even the overlap from the base of a high-abundance peptide ion peak with a lower abundance species may result in poorer quality MS/MS spectra produced from ion activation at the back of the drift tube. In recent studies we have shown that higher-resolution IMS instrumentation leads to decreased spectral overlap resulting in higher-quality MS/MS spectra and increased peptide ion homology scores.[80] In other attempts to increase coverage of low-abundance proteins, we have performed immunoaffinity subtraction of the six most abundant plasma proteins (MARS, Agilent) followed by 2D LC−IMS-MS analysis.[81] These efforts appear to have significantly improved the plasma proteome coverage. Again we note that the MS/MS spectra for all assignments, including those resulting in one-hit protein assignments, have been inspected manually. Despite these efforts, the false positive rate obtained from the reverse protein database search (see above) is likely to have been influenced the most by these single-hit peptides.

One of the advantages of the IMS-MS approach with respect to the determination of false positives is the ability to perform experiments on such short experimental time scales. Identifications obtained from multiple measurements increases the confidence in protein assignments. The use of multiple measurements to substantiate protein assignments is in essence a method of signal averaging the entire proteome. Not only is a high-confidence map derived from multiple measurements required to delineate "change" for comparative proteomics studies but it may also be used to speed dataset feature identification. That is, knowledge of the t_{SCX}, t_R, t_D, and m/z of a feature as well as m/z values for several daughter ions may be sufficient for identification by direct comparison with the map, or after initial identification using lower throughput approaches (e.g., by invoking additional separation stages). Creation of such a searchable map would be a significant

achievement and a large step toward individual plasma profiling.

Comparison with the High-Confidence HUPO Dataset. The high-confidence map has been compared with the high-confidence protein list[36] generated from the HUPO data.[35] Overall, a relatively large number (127) of proteins is observed to overlap with the high-confidence list (compared with the overlap −45 plasma proteins- Anderson and co-workers reported for different sources in 2004[1]). Interestingly, 27 proteins that have been observed with more than one peptide hit are not found in the HUPO high-confidence list. Many of these proteins such as thyroglobulin, melanotransferrin, and apolipoprotein L5 have been confirmed in more recent IMS-MS studies.[81] Additionally, many of the proteins observed with one assigned peptide ion -such as angiopoietin-2, coagulation factor VIII, and plasminogen activator inhibitor 2- have also been confirmed in these more recent studies. It is also intriguing to consider the observed low-abundance proteins not in the HUPO high-confidence list such as alpha fetoprotein, several interleukins, as well as troponin. Again, such comparisons are treated cautiously because of the possibility of false positive assignments (see above).

Because of the large numbers of proteins identified from single hits in the IMS data as well as in the HUPO data,[35,36] *it is difficult to assess the extent to which the two datasets are comparable.* The protein overlap (127) between the two protein lists is comprised mostly of higher abundance plasma proteins. Here we note, however, that this number is larger than the overlap between any two different plasma protein data sources (of 4 total) compiled by Anderson and co-workers.[1] An issue that arises is the significance of the lack of overlap for lower abundance proteins (e.g., many of those arising from one-hit peptide identifications). One reason that there is less overlap of proteins assigned from single peptide identifications may be that such assignments are more likely to be false positives (see above). Separately, the low overlap could result from the disparate instrumentation used for these studies and that used to generate the HUPO data. That is, the type of overlap (contributing to the quality of the MS/MS spectra and thus protein coverage) in analytical dimensions is different for the IMS instrument and conventional LC−MS instrumentation (t_R and t_D versus t_R and m/z, respectively). Additionally, the scanning nature of traditional MS approaches may account for the low protein coverage of some species.[26] Clearly, much work remains to be done with regard to maximizing plasma proteome coverage for all experimental methods.

Experimental Sensitivity and Reproducibility. Ideally, plasma proteomics technology would have the ability to identify peptides from proteins of vastly different concentration (~10^9 to 10^{10} range).[5] With the dynamic range of mass spectrometers (~10^2 to less prevalently 10^5),[82−86] it is difficult to observe very low-abundance species or those of low ionization efficiency (i.e., peptides that produce weak signals) in the presence of higher abundance species. An attractive feature of the current approach is that the mobility dispersion of ions (much like condensed-phase separations) can serve to increase the overall experimental sensitivity and thus the range of protein concentrations that can be addressed in profiling studies. Figure 3 shows the assignment of a peptide from a very low abundance protein (pg·mL^{-1} range). As noted above, such assignments of trace plasma components are treated cautiously because of the possibility to obtain false positive results and, although IMS-MS techniques have previously demonstrated low attomole detection limits from direct infusion experiments,[87] the detection of a cytokine peptide may be difficult requiring subattomole on-column detection limits. The more important issue demonstrated in Figure 3 (compared with the type of assignment) is that the IMS approach offers advantages by removing chemical noise to allow the collection of MS/MS data for species exhibiting comparatively weak ion signals.

In addition to sensitivity and dynamic range requirements, comparative profiling technology must exhibit high reproducibility. To assess the experimental reproducibility, triplicate measurements of a sample obtained from pooled SCX fractions have been performed.[88] Overall 125 proteins have been assigned from 207 peptide ions. Of these, 25 proteins have been observed in more than one replicate analysis. For the most part, the number of peptide ions observed for these proteins do not vary by more than one assignment across the replicate runs. The lone exception shows a difference of two peptides between any two runs. From the 207 peptide ions, 42 high-confidence (using the criteria outlined above) peptide assignments have been analyzed for map position reproducibility. The percent relative uncertainties are determined to be 4.08, 1.87, and 0.02% for the t_R, t_D, m/z measurements, respectively. The relatively high reproducibility at this early stage suggests that IMS-MS measurements are well suited for comparative proteomics studies and improvements are already envisioned to increase the overall experimental reproducibility. For example, a nanoflow LC pumping system and automated sample injection and data acquisition will be implemented. Such minor changes in the instrumentation should lead to higher measurement reproducibility and improved alignment across multiple data sets.

Current Limitations and Future Directions. Although the data reported here demonstrate several advantages of IMS-MS techniques, challenges remain in the development of a robust analytical platform utilizing such instrumentation. Descriptions of a number of challenges as well as recent progress have been outlined in several thoughtful reviews presented by others;[44,45,89] only a brief discussion of several problems is presented here. A challenging problem for the LC−IMS-MS methods described here is the required informatics capabilities. Generally, the rate of data generation is ~0.2−1 GB·min^{-1} for a single LC run. Improving ion trapping efficiency and ion transmission through the drift tube will significantly increase this rate. Such data generation not only requires massive data archival capacity but also powerful data processing, analysis, and database searching capabilities. Ongoing informatics efforts now permit data post-processing and protein database searching of a single LC−IMS-MS run within a few hours and, although such work is still the bottleneck in map generation, current efforts are underway to parallelize the algorithms and the database searching process.

Another limitation, not unique to IMS-MS methods, is the relatively low assignment percentage of observed features. For 10 SCX fractions, there are between 2 and 7 × 10^5 parent ions (2−7 × 10^4 for each fraction). The 6167 peptide assignments that are above the identity cutoff and the fewer assignments (731) in the refined map represent a small fraction (~0.9 to ~3.1% and ~0.1 to ~0.4%, respectively) of the total number of observed features. Several factors may contribute to the relatively low assignment efficiency. Such factors may include the mobility overlap of precursor ions as well as lower quality MS/MS data for many features (e.g., large, stable ions or those from very low-abundance peptides). Several approaches (discussed below) for improving the sensitivity of the instrumentation, the overall experimental resolution, and the data analysis

software are being investigated to increase the percentage of assigned peptides.

Instrumentation design improvements include increased ion storage at the front of the drift tube as well as transmission through the mobility region. The overall trapping efficiency in the ion funnel has recently been determined to be relatively low (~10%). Future efforts will address the ion storage and transmission issues. One approach may be to incorporate the novel "hourglass" ion funnel design described by Smith and co-workers.[90] Also, a number of field-focusing strategies[89−93] for improving ion transmission through the drift tube may be pursued.

Because some coeluting peptide ions are not entirely resolved in the drift dimension, MS/MS datasets may contain undesired peaks. Two corrective approaches are being considered. The first involves instrumental changes that will increase the mobility resolving power. Recent modifications including the quadrupling of the mobility region length have provided a 3 to 4-fold increase in the resolving power.[94−96] The second approach involves software development. As mentioned above, fragment ions are linked to precursors based on t_R and t_D values. This approach does not utilize all the information in the dataset (e.g., the persistence of each feature in the LC dimension). An additional constraint in linking precursors with fragments might match t_R persistence of fragments and precursors. Integrated peak intensities may also be used; fragments with higher integrated intensities than precursor ions will be excluded from their MS/MS dataset.

Conclusions

With the development of mass spectrometry instrumentation over the last 10 years, tremendous progress has been made in the area of plasma proteome characterization. The perceived payoff associated with the ability to profile individual plasma samples has accelerated the development of methodologies that maximize proteome coverage while minimizing overall analysis times. The data presented here, representing the first demonstration of a characterization of the plasma proteome using two-dimensional (2D) LC−IMS-MS methods, suggest that this approach may present an emerging technology for maximizing proteome coverage while minimizing experimental times. Hundreds of LC−IMS-MS dataset features can be identified -many of which have not been identified previously with other methods- and compiled into a high-confidence analytical map from relatively rapid analyses. These short experimental time scales, afforded by the dispersive nature of the IMS approach, will allow greater sampling of the plasma proteome leading to even higher-confidence plasma proteome maps *generated with IMS-MS techniques* in the future. Additionally, the ability to rapidly analyze individual samples (for comparison against such high-confidence maps) will bolster plasma profiling efforts where plasma from large numbers of individuals can be characterized in a reasonable amount of time. *The ability to profile large populations of individuals would enhance plasma biomarker discovery efforts.*

Acknowledgment. We are grateful to the reviewers for helpful insights regarding the work presented here. This work is supported in part by grants from the NIH (AG-024547, P41-RR018942, and 1R43HL082382), the Indiana 21st Century fund, and funds from the METACyte initiative (funded by the Lilly Endowment), Pacific Northwest National Laboratory (PNNL) efforts supported by NIH National Center for Research Resources (RR 18522), and the Environmental Molecular Science Laboratory. PNNL is operated by Battelle Memorial Institute for the U.S. Department of Energy under contract DE-AC06-76RLO-1830. Disclosure of conflicts: Three of the authors (S.J.V., S.N., and D.E.C.) are founders of Predictive Physiology and Medicine (PPM). At the time that this article was written, D.E.C. (a professor at Indiana University) served as the interim CEO. S.J.V. is a full-time employee of PPM.

Supporting Information Available: Complete list of the high-confidence proteins as well as the number of peptide ions observed for each of the 731 unique peptide ion assignments (438 proteins) from protein database searches using the LC−IMS-MS data. This material is available free of charge via the Internet at http://pubs.acs.org.

References

(1) Anderson, N. L.; Polanski, M.; Pieper, R.; Gatlin, T.; Tirumalai, R. S.; Conrads, T. P.; Veenstra, T. D.; Adkins, J. N.; Pounds, J. G.; Fagan, R.; Lobley, A. *Mol. Cell. Proteomics* **2004**, *3.4*, 311.
(2) Omenn, G. S. *Proteomics* **2004**, *4*, 1235.
(3) Morel, N. M.; Holland, J. M.; van der Greef, J.; Marple, E. W.; Clish, C.; Loscalzo, J.; Naylor, S. *Mayo Clin. Proc.* **2004**, *79*, 651.
(4) Putnam, F. W., Ed. *The Plasma Proteins: Structure, Function and Genetic Control*; Academic Press: New York, 1975.
(5) Anderson, N. L.; Anderson, N. G. *Mol. Cel. Proteomics* **2002**, *1*, 845.
(6) Kennedy, S. *Toxicol. Lett.* **2001**, *120*, 379.
(7) Petricoin, E. F.; Ardekani, A. M.; Hitt, B. A.; Levine, P. J.; Fusaro, V. A.; Steinberg, S. M.; Mills, G. B.; Simone, C.; Fishman, D. A.; Kohn, E. C.; Liotta, L. A. *Lancet* **2002**, *359*, 572.
(8) Cottingham, K. *Anal. Chem.* **2003**, *75*, 472A.
(9) Li, J.; White, N.; Zhang, Z.; Rosenzweig, J.; Mangold, L. A.; Partin, A. W.; Chan, D. W. *J. Urology* **2004**, *171*, 1782.
(10) Petricoin, E. F.; Liotta, L. A. *Curr. Opin. Biotechnol.* **2004**, *15*, 24.
(11) Weston, A. D.; Hood, L. *J. Proteome Res.* **2004**, *3*, 179.
(12) Zhang, H.; Yan, W.; Aebersold, R. *Curr. Opin. Chem. Biol.* **2004**, *8*, 66.
(13) Diamandis, E. P. *Lancet* **2002**, *360*, 170.
(14) Diamandis, E. P. *J. Natl. Cancer Inst.* **2003**, *95*, 489.
(15) Diamandis, E. P. *Clin. Chem.* **2003**, *49*, 1272.
(16) Anderson, L.; Anderson, N. G. *Proc. Natl. Acad. Sci. U.S.A.* **1977**, *74*, 5421.
(17) Anderson, N. L.; Anderson, N. G. *Electrophoresis* **1991**, *12*, 883.
(18) Ueno, I.; Sakai, T.; Yamaoka, M.; Yoshida, R.; Tsugita, A. *Electrophoresis* **2000**, *21*, 1832.
(19) Pieper, R.; Gatlin, C. L.; Makusky, A. J.; Russo, P. S.; Schatz, C. R.; Miller, S. S.; Su, Q.; McGrath, A. M.; Estock, M. A.; Parmar P. P.; Zhao, M.; Huang, S. T.; Zhou, J.; Wang, F.; Esquer-Blasco, R.; Anderson, N. L.; Taylor, J.; Steiner, S. *Proetomics* **2003**, *3*, 1345.
(20) Washburn, M. P.; Wolters, D.; Yates, J. R. III. *Nat. Biotechnol.* **2001**, *19*, 242.
(21) Wolters, D. A.; Washburn, M. P.; Yates, J. R. *Anal. Chem.* **2001**, *73*, 5683.
(22) Peng, J.; Elias, J. E.; Thoreen, C. C.; Licklider, L. J.; Gygi, S. P. *J. Proteome Res.* **2003**, *2*, 43.
(23) Adkins, J. N.; Varnum, S. M.; Auberry, K. J.; Moore, R. J.; Angell, N. H.; Smith, R. D.; Springer, D. L.; Pounds, J. G. *Mol. Cell. Proteomics* **2002**, *1*, 947.
(24) Tirumalai, R. S.; Chan, K. C.; Prieto, D. A.; Issaq, H. J.; Conrads, T. P.; Veenstra, T. D. *Mol. Cell Proteomics* **2003**, *2*, 1096.
(25) Wu, S. L.; Choudhary, G.; Ramstrom, M.; Bergquist, J.; Hancock, W. S. *J. Proteome Res.* **2003**, *2*, 383.
(26) Shen, Y.; Jacobs, J. M.; Camp, D. G. II, Fang, R.; Moore, R. J.; Smith, R. D.; Xiao, W.; Davis, R. W.; Tompkins, R. G. *Anal. Chem.* **2004**, *76*, 1134.
(27) Zhou, M.; Lucas, D. A.; Chan, K. C.; Issaq, H. J.; Petricoin, E. F.; Liotta, L. A.; Veenstra, T. D.; Conrads, T. R. *Electrophoresis* **2004**, *25*, 1289.
(28) Mehta, A. I.; Ross, S.; Lowenthal, M. S.; Fusaro, V.; Fishman, D. A.; Petricoin, E. F.; Liotta, L. A. *Dis. Markers* **2003**, *19*, 1.
(29) Zhang, H.; Li, X−j.; Martin, D. B.; Aebersold, R. *Nat. Biotechnol.* **2003**, *21*, 660.
(30) Anderson, N. L.; Anderson, N. G.; Haines, L. R.; Hardie, D. B.; Olafson, R. W.; Pearson, T. W. *J. Proteome Res.* **2004**, *3*, 235.
(31) Nedelkov, D.; Tubbs, K. A.; Niederkofler, E. E.; Kiernan, U. A.; Nelson, R. W. *Anal. Chem.* **2004**, *76*, 1733.
(32) Rodriguez-Pineiro, A. M.; Ayude D.; Rodriguez-Berrocal F. J.; de la Cadena, M. P. *J. Chromatogr. B* **2004**, *803*, 337.

(33) Hagglund, P.; Bunkenborg, J.; Elortza, F.; Jensen, O. N.; Roepstorff, P. *J. Proteome Res.* **2004**, *3*, 556.
(34) For reports of recent results for human plasma proteomics studies using different analytical methods see the 2005 issue 13 of the journal *Proteomics*. The entire issue contains reports of results from HUPO's Plasma Proteome Initiative.
(35) Omenn, G. S.; et al. *Protoemics* **2005**, *5*, 3226.
(36) States, D. J.; Omen, G. S.; Blackwell, T. W.; Fermin, D.; Speicher D. W.; Hanash, S. M. *Nat. Biotechnol.* **2006**, *24*, 333.
(37) Valentine, S. J.; Counterman, A. E.; Hoaglund, C. S.; Reilly, J. P.; Clemmer, D. E. *J. Am. Soc. Mass Spectrom.* **1998**, *9*, 1213.
(38) Henderson, S. C.; Valentine, S. J.; Counterman, A. E.; Clemmer, D. E. *Anal. Chem.* **1999**, *71*, 291.
(39) Ruotolo B. T.; Gillig, K. J.; Stone, E. G.; Russell, D. H. *J. Chromat. B* **2002**, *782*, 385.
(40) Brandon, B. T.; Gillig, K. J.; Stone, E. G.; Russell, D. H.; Fuhrer, K.; Gonin, M.; Schultz, J. A. *Int. J. Mass Spectrom.* **2002**, *219*, 253.
(41) Steiner W. E.; Clowers, B. H.; English, W. A.; Hill, H. H. *Rapid Comm. Mass Spectrom.* **2004**, *18*, 882.
(42) Moon, M. H.; Myung, S.; Plasencia, M.; Hilderbrand, A. E.; Clemmer, D. E. *J. Proteome Res.* **2003**, *2*, 589.
(43) For a discussion of the peak capacity of LC−IMS-MS methods for protein digests see: Valentine, S. J.; Kulchania, M.; Srebalus Barnes, C. A.; Clemmer, D. E. *Int. J. Mass Spectrom.* **2001**, *212*, 97−109.
(44) Liu, X.; Plasencia, M.; Ragg, S.; Valentine, S. J.; Clemmer, D. E. *Brief Funct. Genomic Proteomic* **2004**, *3*, 177−186.
(45) Valentine, S. J.; Liu, X.; Plasencia, M. D.; Hilderbrand, A. E.; Kurulugama, R. T.; Koeniger, S. L.; Clemmer, D. E. *Expert Rev. Proteomics* **2005**, *2*, 553−565.
(46) Counterman, A. E.; Hilderbrand, A. E.; Srebalus Barnes, C. A.; Clemmer, D. E. *J. Am. Soc. Mass Spectrom.* **2001**, *12*, 1020.
(47) Taraszka, J. A.; Counterman, A. E.; Clemmer, D. E. *Fresenius J. Anal. Chem.* **2001**, *369*, 234.
(48) Hoaglund-Hyzer, C. S.; Li, J.; Clemmer, D. E. *Anal. Chem.* **2000**, *72*, 2737.
(49) Hunter, J.; Fye, J.; Jarrold, M. F. *Science* **1993**, *260*, 784.
(50) Hunter, J. M.; Jarrold, M. F. *J. Am. Chem. Soc.* **1995**, *117*, 10317.
(51) Clemmer, D. E.; Hudgins, R. R.; Jarrold, M. F. *J. Am. Chem. Soc.* **1995**, *117*, 10141.
(52) Wyttenbach, T.; von Helden, G.; Bowers, M. T. *J. Am. Chem. Soc.* **1996**, *118*, 8355.
(53) Counterman, A. E.; Clemmer, D. E. *J. Am. Chem. Soc.* **2001**, *123*, 1490.
(54) Badman, E. R.; Hoaglund-Hyzer, C. S.; Clemmer, D. E. *Anal. Chem.* **2001**, *73*, 6000.
(55) St. Louis, R. H.; Hill, H. H. *Crit. Rev. Anal. Chem.* **1990**, *21*, 321.
(56) Clemmer, D. E.; Jarrold, M. F. *J. Mass Spectrom.* **1997**, *32*, 577.
(57) Hoaglund Hyzer, C. S.; Counterman, A. E.; Clemmer, D. E. *Chem. Rev.* **1999**, *99*, 3037.
(58) Collins, D. C.; Lee, M. L. *Anal. Bioanal. Chem.* **2002**, *372*, 66.
(59) Wyttenbach, T.; Bowers, M. T. *Mod. Mass Spectrom. Top. Curr. Chem.* **2003**, *225*, 207.
(60) Valentine, S. J.; Koeniger, S. L.; Clemmer, D. E. *Anal. Chem.* **2003**, *75*, 6202.
(61) Taraszka, J. A.; Kurulugama, R.; Sowell, R.; Valentine, S. J.; Koeniger, S. L.; Arnold, R. J.; Miller, D. F.; Kaufman, T. C.; Clemmer, D. E. *J. Proteome Res.* **2005**, *4*, 1223.
(62) Shaffer, S. A.; Prior, D. C.; Anderson, G. A.; Udseth, H. R.; Smith, R. D. *Anal. Chem.* **1998**, *70*, 4111.
(63) Him, T.; Tolmachev, A. V.; Harkewicz, R.; Prior, D. C.; Anderson, G.; Udseth, H. R.; Smith, R. D.; Bailey, T. H.; Rakov, S.; Futrell, J. H. *Anal. Chem.* **2000**, *72*, 2247.
(64) Mason, E. A.; McDaniel, E. W. *Transport Properties of Ions in Gases*; Wiley: New York, 1988.
(65) Valentine, S. J.; Counterman, A. E.; Hoaglund, C. S.; Reilly, J. P.; Clemmer, D. E. *J. Am. Soc. Mass Spectrom.* **1998**, *9*, 1213.
(66) Taraszka, J. A.; Counterman, A. E.; Clemmer, D. E. *Fresenius J. Anal. Chem.* **2001**, *369*, 234.
(67) Hoaglund-Hyzer, C. S.; Li, J.; Clemmer, D. E. *Anal. Chem.* **2000**, *72*, 2737.
(68) All research was carried out using an approved protocol by the Indiana University Human Subjects Committee (#04−9243).
(69) Hoaglund, C. S.; Valentine, S. J.; Sporleder, C. R.; Reilly, J. P.; Clemmer, D. E. *Anal. Chem.* **1998**, *70*, 2236.
(70) Valentine, S. J.; Kulchania, M.; Srebalus Barnes, C. A.; Clemmer, D. E. *Int. J. Mass Spectrom.* **2001**, *212*, 97.
(71) Taraszka, J. A.; Gao, X.; Valentine, S. J.; Sowell, R. A.; Koeniger, S. L.; Miller, D. F.; Kaufman, T. C.; Clemmer, D. E. *J. Proteome Res.* **2005**, *4*, 1238.
(72) Available at ftp://us.expasy.org/databases/swiss-prot/.
(73) Cargile, B. J.; Bundy, J. L.; Stephenson, J. L. Jr. *J. Proteome Res.* **2004**, *3*, 1082.
(74) Valentine, S. J.; Counterman, A. E.; Hoaglund-Hyzer, C. S.; Clemmer, D. E. *J. Phys. Chem. B* **1999**, *103*, 1203.
(75) Valentine, S. J.; Counterman, A. E.; Clemmer, D. E. *J. Am. Soc. Mass Spectrom.* **1999**, *10*, 1188.
(76) Lochmüller, C. H.; Reese, C.; Aschman, A. J. *J. Chromatogr. A* **1993**, *656*, 3.
(77) Petritis, K.; Kangas, L. J.; Ferguson, P. L.; Anderson, G. A.; Paša-Tolić, L.; Lipton, M. S.; Auberry, K. J.; Strittmatter, E. F.; Shen, Y.; Zhao, R.; Smith, R. D. *Anal. Chem.* **2003**, *75*, 1039.
(78) We note that the selection of ±0.1 Da. is not limited by the resolving power or mass accuracy (~4500 and 20−50 ppm, respectively) of the home-built TOF instrument. The wider selection has been used to allow for sampling of very low-abundance fragment ions (i.e., ions in such low abundance that "statistically significant" TOF peak distributions are not obtained). Again, the mobility dispersion allows the classification of clusters of low-intensity bins as signal because they are removed from interfering chemical noise. Overall, from careful examination of random false positive assignments as well as classical plasma protein assignments, the wider range does not significantly increase false positive rates.
(79) The reverse protein database was generated by inverting the protein sequences in the Swiss-Prot protein database.
(80) Valentine, S. J.; Koeniger, S. L.; Merenbloom, S. I.; Knierman, M.; Hale, J.; Clemmer, D. E. In preparation.
(81) Liu, X.; Plasencia, M. D.; Valentine, S. J.; March, K. L.; Clemmer, D. E. In preparation.
(82) Bruce, J. E.; Anderson, G. A.; Smith, R. D. *Anal. Chem.* **1996**, *68*, 534.
(83) Cargile, B. J.; Bundy, J. L.; Grunden, A. M.; Stephenson, J. L., Jr. *Anal. Chem.* **2004**, *76*, 86.
(84) Technical notes for Agilent LC MSD TOF http://www.chem.agilent.com/temp/radA4BAE/00042009.pdf.
(85) Thermo Electron Corporation Application Notes http://www.thermo.com/eThermo/CMA/PDFs/Articles/articlesFile_21825.pdf.
(86) Thermo Electron Corporation Application Notes http://www.thermo.com/eThermo/CMA/PDFs/Articles/articlesFile_23993.pdf.
(87) Myung, S.; Lee, Y. L.; Moon, M. H.; Taraszka, J. A.; Sowell, R.; Koeniger, S. L.; Hilderbrand A. E.; Valentine, S. J.; Cherbas, L.; Cherbas, P.; Kaufmann, T. C.; Miller, D. F.; Mechref, Y.; Novotny, M. V.; Ewing, M.; Clemmer D. E. *Anal. Chem.* **2003**, *75*, 5137.
(88) Here we do not assess the coefficient of variation (CV) in the intensities of these identified features because the LC injection was performed manually and is likely to result in significant variation. Additionally, the home-built TOF detector has a tendency to saturate at relatively low peptide concentrations because of the ion "bunching" caused by the mobility separation. Current instrumental efforts involve the coupling of an LC system with an autosampler as well as the installation of a commercial TOF detector (and the development of an analogue detection scheme). Although the successful implementation of these improvements will enhance the ability to determine accurate CVs for peptide ion intensity, we note that the reproducibility studies described in the text are aimed at determining the ability to align two different datasets (necessary for comparative mapping studies).
(89) McLean, J. A.; Ruotolo, B. T.; Gillig, K. J.; Russell, D. H. *Int. J. Mass Spectrom.* **2005**, *240*, 301.
(90) Tang, K.; Shvartsburg, A. A.; Lee, H. N.; Prior, D. C.; Buschbach, M. A.; Li, F.; Tolmachev, A.; Anderson, G. A.; Smith, R. D. *Anal. Chem.* **2005**, *77*, 3330.
(91) Lee, Y. J.; Hoaglund-Hyzer, C. S.; Taraszka, J. A.; Zientara, G. A.; Counterman, A. E.; Clemmer, D. E. *Anal. Chem.* **2001**, *73*, 3549.
(92) Gillig, K. J.; Ruotolo, B.; Stone, E. G.; Russell, D. H.; Fuhrer, K.; Gonin, M.; Schultz, A. J. Coupling High-Pressure MALDI with Ion Mobility/Orthogonal Time-of-Flight Mass Spectrometry. *Anal. Chem.* **2000**, *72*, 3965.
(93) Gillig, K. J.; Ruotolo, B. T.; Stone, E. G.; Russell, D. H. *Int. J. Mass Spectrom.* **2004**, *239*, 43.
(94) Koeniger, S. L.; Merenbloom, S. I.; Clemmer, D. E. *J. Phys. Chem.* **2006**, *110*, 7017.
(95) Merenbloom, S. I.; Koeniger, S. L.; Valentine, S. J.; Plasencia, M. D.; Clemmer, D. E. *Anal. Chem.* **2006**, *78*, 2802.
(96) Koeniger, S. L.; Merenbloom, S. I.; Valentine, S. J.; Udseth, H.; Smith, R.; Clemmer, D. E. *Anal. Chem.* **2006**, *78*, 4161.

PR060232I